ISSN 0036-0295, Russian Metallurgy (Metally), Vol. 2015, No. 4, pp. 317–323. © Pleiades Publishing, Ltd., 2015.
Original Russian Text © M.S. Belyaev, V.F. Terent'ev, M.M. Bakradze, M.A. Gorbovets, M.A. Gol'dberg, 2014, published in Deformatsiya i Razrushenie Materialov, 2014, No. 7, pp. 27–33.

APPLIED PROBLEMS OF STRENGTH AND PLASTICITY

Low-Cycle Fatigue of a VZh175 High-Temperature Alloy under Elastoplastic Deformation Conditions

M. S. Belyaev[a], V. F. Terent'ev[b], M. M. Bakradze[a], M. A. Gorbovets[a], and M. A. Gol'dberg[b]

[a] *FGUP VIAM, Moscow, 105005 Russia*

[b] *Baikov Institute of Metallurgy and Materials Science, Russian Academy of Sciences, Leninskii pr. 49, Moscow, 119991 Russia*

e-mail: fatig@mail.ru

Received February 24, 2014

Abstract—The low-cycle fatigue of a VZh175 nickel superalloy is studied under conditions of complete deformation per loading cycle at an initial cycle asymmetry $R = 0$, a deformation amplitude $\varepsilon_a = 0.4–0.6\%$, and a temperature of 20 and 650°C. The specific features of cyclic hardening/softening of the alloy under these conditions are detected. The mechanisms of fatigue crack nucleation and growth are analyzed as functions of the deformation amplitude and the test temperature.

DOI: 10.1134/S0036029515040023

INTRODUCTION

Low- and high-cycle fatigue is an important characteristic of metals and alloys, since it inferences the service life of severely loaded parts and constructions [1–4]. Precipitation-hardening nickel-based superalloys, which are intended for producing the structural members of gas turbine engines, have attracted the particular attention of researchers. These alloys are characterized by a complex alloying system, are hardened by the intermetallic γ' phase of a complex composition, and contain disperse carbide and boride phases [5–11]. Although the low-cycle fatigue of next-generation nickel-based superalloys was studied in many works [12–18], some aspects related to the influence of the structural state on the new precipitation-hardening nickel superalloys and their low-cycle fatigue are still poorly understood.

The purpose of this work is to study the low-cycle fatigue of a VZh175 superalloy, which is used in a gas turbine engine under various loading conditions, namely, various deformation temperatures and temperatures.

EXPERIMENTAL

A VZh175 alloy (Ni base; alloying elements Co, Cr, W, Mo, Al, Ti, Nb, C) was studied. In the initial state, its structure was represented by γ solid solution grains 15–25 μm in size, and primary γ'-phase particles 2–7 μm in size and hardening (Nb,Ti)C carbides and $(Mo,Cr,W,Co)_3B_2$ borides were located along grain boundaries (Fig. 1a). Hardening inclusions of the secondary and tertiary γ' phases of composition $(Ni,Co,Cr)_3(Al,Ti,Nb,Mo,W,V)$ 10–700 nm in size were detected inside the grains (Fig. 1b) [19]. The mechanical properties of the alloy determined upon static tension are given in Table 1.

Low-cycle fatigue tests consisted in uniaxial cyclic tension–compression of smooth cylindrical specimens 5.0 mm in diameter with a gage length of 15 mm using a servohydraulic LFV-100 machine at a constant total (elastic and plastic) deformation per loading

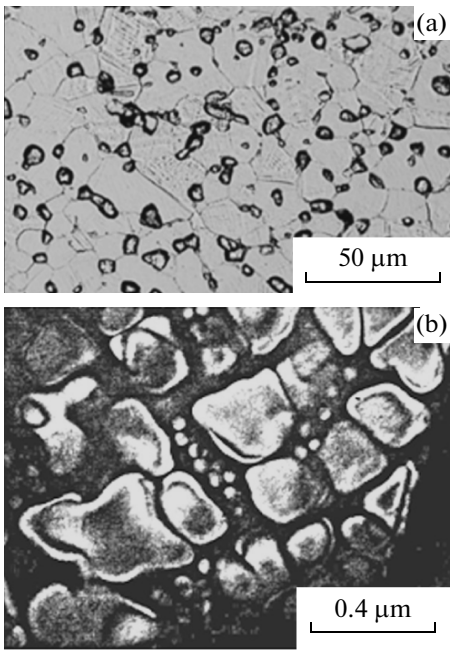

Fig. 1. (a) Structure and (b) substructure of VZh175 alloy.

Table 1. Mechanical properties of VZh175 alloy

T, °C	σ_u, MPa	$\sigma_{0.2}$, MPa	δ, %
20	1600	1190	14
650	1530	1080	12

cycle at a frequency $\nu = 1$ Hz and a deformation asymmetry coefficient $R_\varepsilon = 0$ in an initial cycle. Mechanical hysteresis loops were recorded with an Epsilon extensimeter having a gage length of 12.5 mm. The series of experiments differed in the total strain amplitude per loading cycle (ε_a = 0.4–0.6%) and temperature (20, 650°C). The time to failure was $N_f = (1–13) \times 10^3$ cycles (Table 2).

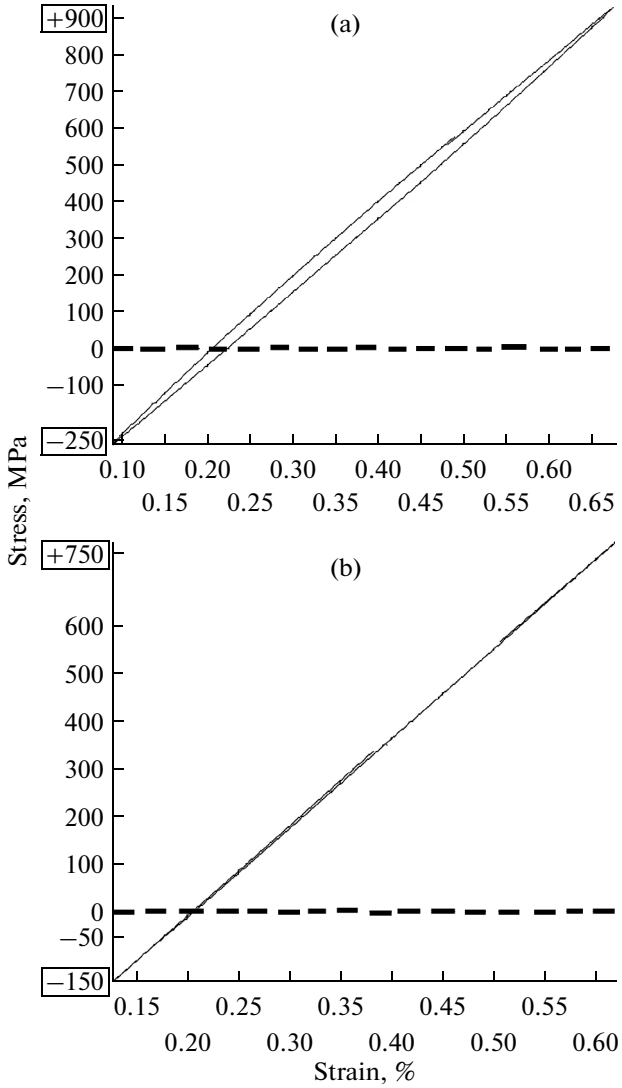

Fig. 2. Mechanical hysteresis loops of the VZh175 alloy subjected to low-cycle tests at $\varepsilon_a = 0.4$, $N = 5$ cycles, and T = (a) 20 and (b) 650°C.

Table 2. Results of low-cycle fatigue tests of VZh175 alloy

Parameter	Test temperature, °C					
	20	20	650	650	650	650
ε_a, %	0.6	0.4	0.5	0.5	0.4	0.4
N_f, cycles	2483	10251	894	1040	4222	13063

RESULTS AND DISCUSSION

A nonstationary change in the cycle shape and continuous formation of an asymmetric tension–compression cycle are detected at the chosen initial regime of low-cycle elastoplastic deformation with a cycle asymmetry $R_\varepsilon = 0$ during the first $N = 100$ cycles. The average cycle stress is always located in the range of tensile stresses. As an example, Fig. 2 shows the mechanical hysteresis loops recorded in $N = 5$ cycles at $\varepsilon_a = 0.4\%$ and various test temperatures. It should be noted that the compressive stresses at the beginning of loading are relatively low, 250 and 150 MPa for test temperatures of 20 and 650°C, respectively. After $N =$ 20 cycles, they are 400 and 350 MPa, respectively. When a stationary deformation cycle regime is reached, the difference between the tensile and compressive stresses in one cycle decreases substantially. Nevertheless, the average cycle stress is always in the range of tensile stresses.

Figure 3 shows the typical mechanical hysteresis loops of VZh175 alloy specimens tested up to $N = 1/2N_f$ at $\varepsilon_a = 0.4\%$ and temperatures of 20 and 650°C (under the chosen conditions, the difference in the numbers of cycles to failure is insignificant). Note a

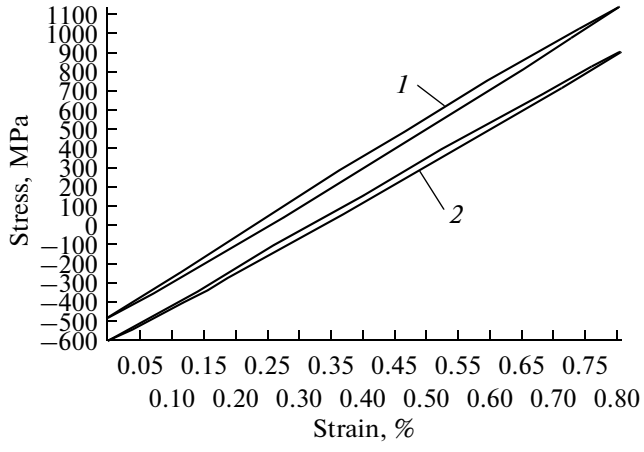

Fig. 3. Mechanical hysteresis loops of the VZh175 alloy subjected to low-cycle tests at $\varepsilon_a = 0.4$ and fatigue lifetime $N = 1/2N_f$: (*1*) $T = 20$°C, $N = 5100$ cycles; (*2*) $T = 650$°C, $N = 6500$ cycles.

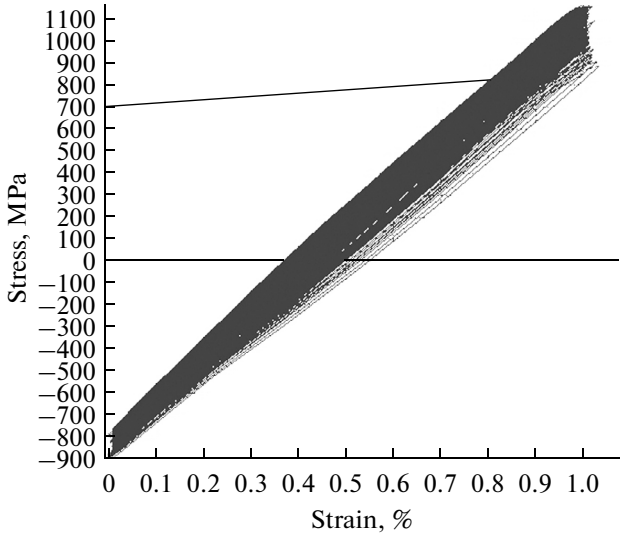

Fig. 4. Mechanical hysteresis loops of the VZh175 alloy subjected to low-cycle tests at $\varepsilon_a = 0.5\%$, $T = 650$°C, and $N_f = 1040$ cycles.

slightly higher slope of the mechanical hysteresis loop to the deformation axis under the test conditions at room temperature. Moreover, the strain accumulated at room temperature is $\varepsilon_{ac} = 0.03\%$, which is slightly higher than the strain accumulated at 650°C ($\varepsilon_{ac} = 0.02\%$). Figure 4 shows the kinetics of mechanical hysteresis loops at $\varepsilon_a = 0.5\%$ and a test temperature of 650°C ($N_f = 1040$ cycles).

When comparing the cyclic hardening/softening curves of the VZh175 alloy tested at $\varepsilon_a = 0.4\%$, we were able to detect a certain increase in the maximum cyclic tensile stress at $N = 3 \times 10^3$ cycles and a loading temperature of 20°C (Fig. 5a). Then, the maximum tensile stress and the minimum compressive stress decrease up to failure; that is, cyclic softening takes place. At a test temperature of 650°C, the maximum and minimum stresses remain stable (1050 and 450 MPa, respectively) up to $N = 2 \times 10^3$ cycles, and sharp softening then occurs (Fig. 5b). The beginning of sharp softening during low-cycle fatigue tests at constant ε_a is related to the appearance of a fatigue crack [20].

A slightly different picture is observed during tests at higher deformation amplitudes. At $\varepsilon_a = 0.6\%$ and room temperature, the maximum cyclic tensile stress decreases continuously after $N \approx 80$ cycles, and the compressive stress first reaches 1000 MPa and then decreases insignificantly up to failure (Fig. 6a). At a temperature of 650°C and $\varepsilon_a = 0.5\%$ after $N \approx 120$ loading cycles, the tensile stresses also decrease continuously (Fig. 6b), but this decrease is less intense than that at $\varepsilon_a = 0.6\%$ and room temperature (see Fig. 6a). The compressive stresses reach 680 MPa and then decrease continuously up to failure (see Fig. 6b).

Thus, the tensile stresses reach a maximum and then decrease continuously in $N \approx 100$ cycles at high

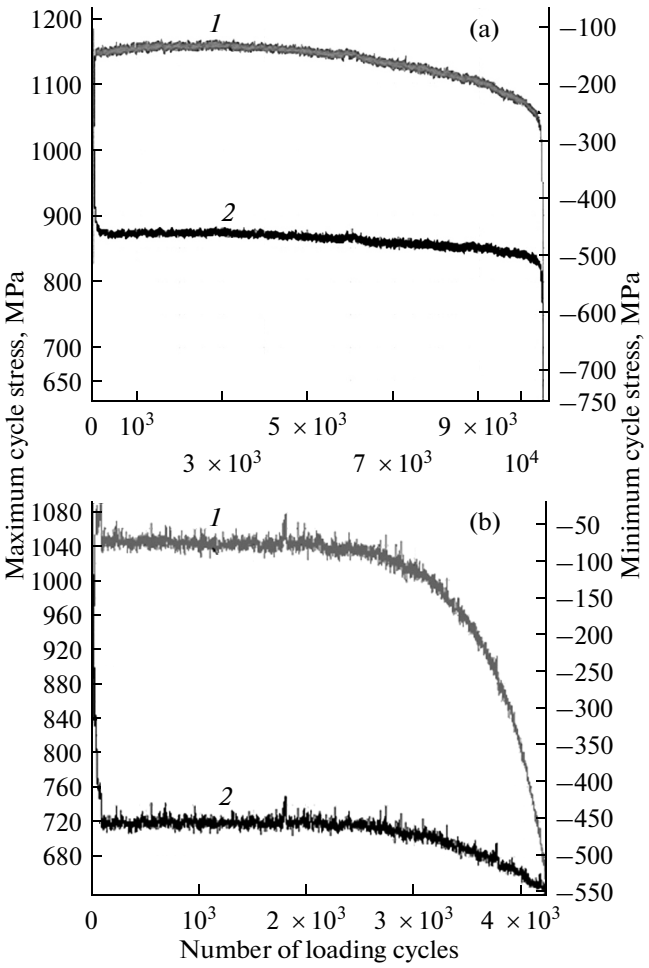

Fig. 5. Cyclic hardening/softening curves of VZh175 alloy specimens tested at $\varepsilon_a = 0.4\%$: (a) $T = 20$°C, $N_f = 10275$ cycles; (b) $T = 650$°C, $N_f = 4222$ cycles. (*1*) Maximum tensile stresses and (*2*) minimum compressive stresses.

elastoplastic deformation amplitudes ($\varepsilon_a = 0.6, 0.5\%$) and all test temperatures. Here, the compressive stresses change ambiguously: they either increase (at 650°C) or decrease (at 20°C) as the number of test cycles increases after the end of a nonstationary segment ($N \approx 100$ cycles). In both cases, the compressive stresses change gradually.

It is interesting to compare the stresses that appear in the alloy at the same deformation amplitude and different test temperatures. For comparison, we chose the samples tested at $\varepsilon_a = 0.4\%$ and withstood a large number of cycles to failure, namely, 10500 and 13000 cycles at 20 and 650°C, respectively (Table 3). It was found that, depending on the test temperature, the stresses in a specimen have different values and peak-to-peak amplitudes after the initial loading segment ($N \approx 100$ cycles). The difference in the peak-to-peak amplitudes is relatively small, 1610 and 1530 MPa at 20 and 650°C, respectively. The difference in the maximum tensile

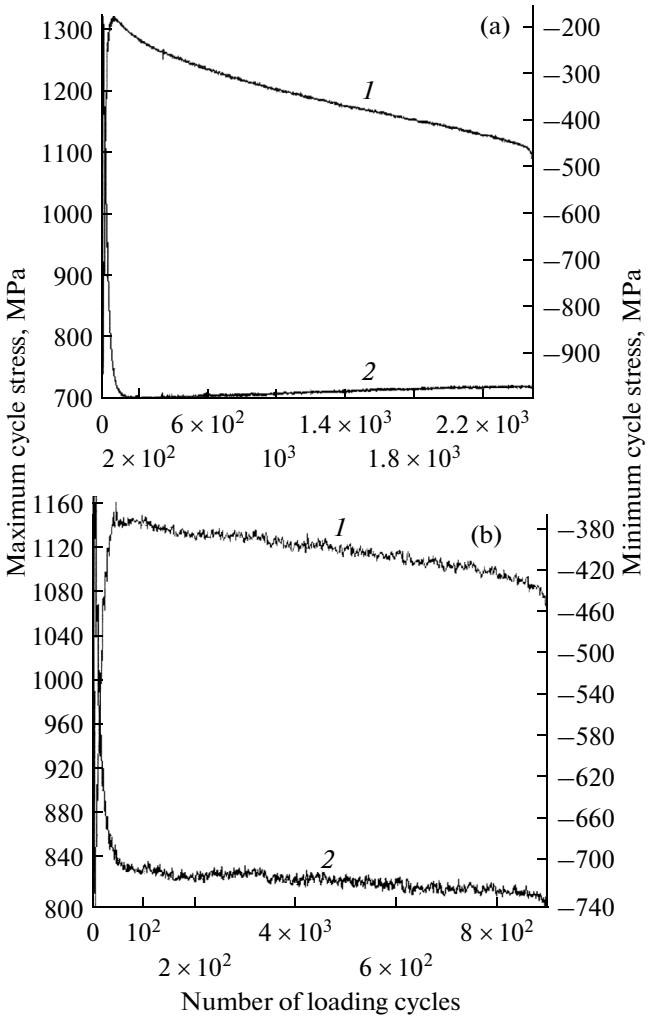

Fig. 6. Cyclic hardening/softening curves of VZh175 alloy specimens: (a) $\varepsilon_a = 0.6\%$, $T = 20°C$, and $N_f = 2483$ cycles; (b) $\varepsilon_a = 0.5\%$, $T = 650°C$, and $N_f = 894$ cycles. (*1*) Maximum tensile stresses and (*2*) minimum compressive stresses.

Table 3. Effect of the test temperature on the stresses appearing in a specimen at a deformation amplitude ε_a = 0.4%

N, 10^3 cycles	Stress, MPa, at temperature			
	20°C		650°C	
0.1	1150*	−460**	930*	−600**
5	1150	−480		
6	1140	−480		
7	1130	−485		
8	1120	−485		
9	1120	−490		
10	1125	−500		
11	Failure	Failure		
12			920	
13			910	−620

* Tensile stresses.
** Compressive stresses.

and compressive stresses is more significant, namely, 200 and 115 MPa at 20 and 650°C, respectively. The average stress in both cases is positive, 325 and 115 MPa, respectively.

When studying the fracture surfaces of VZh175 alloy specimens, we found that the mechanism of their low-cycle fatigue fracture at 20°C weakly depends on the deformation amplitude: a rather rough ductile character of fracture, which is caused by a polycrystalline structure of the material, is detected in all cases. A microcrack nucleates from several sources (Fig. 7a). The zone of initial fatigue crack propagation is characterized by a developed ductile fracture character with ridges and fatigue grooves (Fig. 7b). The zone of stable crack growth has a pronounced groove relief, and the direction of fatigue crack propagation across grooves changes as a function of the orientation of matrix grains (Fig. 7c). The accelerated development of fatigue cracks and static rupture are related to developed ductile fracture (Fig. 7d).

The fracture surfaces of the specimens tested at 650°C and the same deformation amplitude (ε_a = 0.4%) have the main zone of fatigue crack nucleation, from which ridges with fatigue grooves move (Fig. 8a). We studied two specimens under these loading conditions: one specimen withstood 4222 cycles to failure and the other specimen, 13063 cycles. In the former case, a crack nucleated from hardening-phase particles on the specimen surface (Fig. 8a); in the latter case, a crack nucleated from the surface of brittle cleavage, which was likely to form due to the fracture of carbide (Fig. 8b). As in the case of room temperature, the zone of initial crack development has a ductile groove relief with fatigue grooves elongated in the direction of fatigue crack propagation (Fig. 8c). Secondary cracking is observed along fatigue grooves, which can be caused by partial embrittlement of the alloy at the test temperature. The accelerated development of a fatigue crack is related to ductile fracture, and the static rupture surface consists of ductile and quasi-brittle fracture areas (Fig. 8d).

As at $\varepsilon_a = 0.4\%$, the fracture surface at a deformation amplitude $\varepsilon_a = 0.5\%$ and a temperature of 650°C (1040 cycles to failure) has a pronounced zone of fatigue crack nucleation and a zone of stable crack growth (Fig. 9a). A ductile relief with fatigue grooves and microcracks between them is observed near the crack nucleation zone (Fig. 9b). The stage of stable crack growth corresponds to a specific structure in the form of elongated plates or plateaus, between which cracks are observed in some cases. Aggregates of carbides are also visible (Fig. 9c). The fracture in the section of accelerated crack growth is mainly ductile (Fig. 9d).

Thus, the fracture during low-cycle elastoplastic deformation at room temperature is mainly ductile with the presence of typical fatigue grooves. At a test temperature of 650°C, the fracture mechanism is mixed, namely, ductile and quasi-brittle.

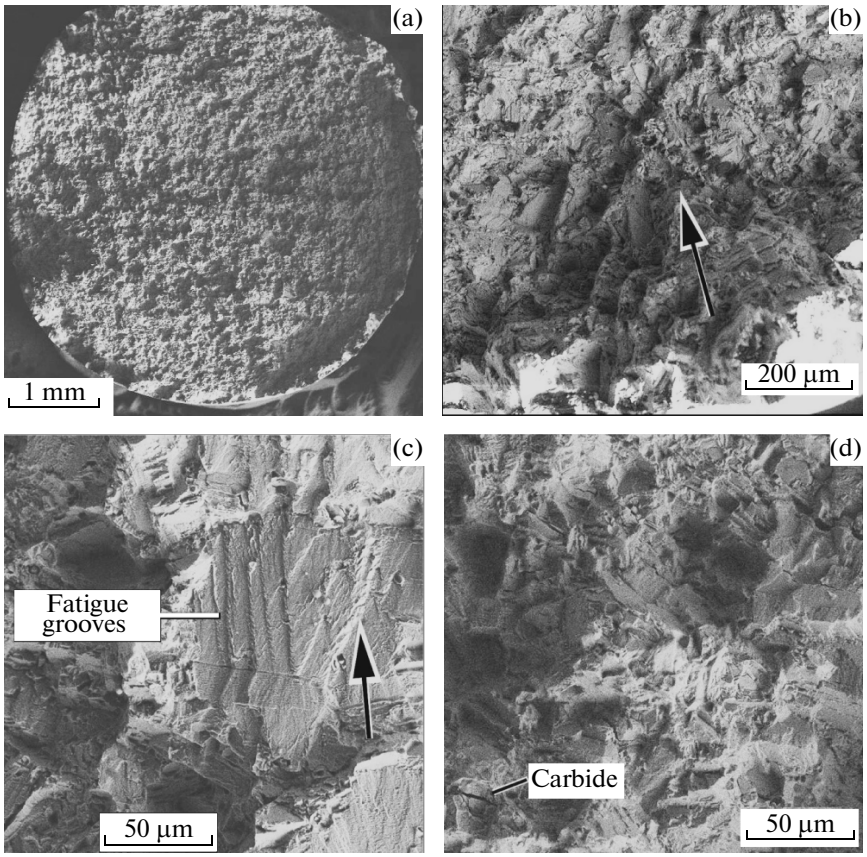

Fig. 7. Fatigue fracture surfaces of the VZh175 alloy at $T = 20°C$: (a, d) $\varepsilon_a = 0.6\%$, $N_f = 2483$ cycles; (b, c) $\varepsilon_a = 0.4\%$, $N_f = 10251$ cycles. The arrows indicate the direction of fatigue crack development.

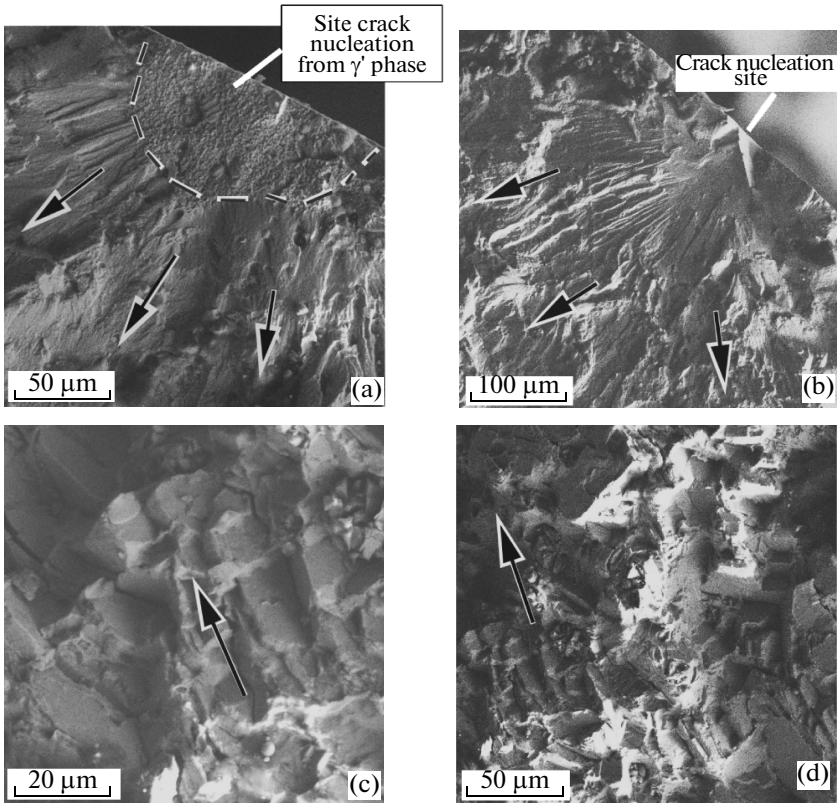

Fig. 8. Fatigue fracture surfaces of the VZh175 alloy at $T = 650°C$, $\varepsilon_a = 0.4\%$, and (a) $N_f = 4222$ cycles and (b–d) $N_f = 13063$ cycles. The arrows indicate the direction of fatigue crack development.

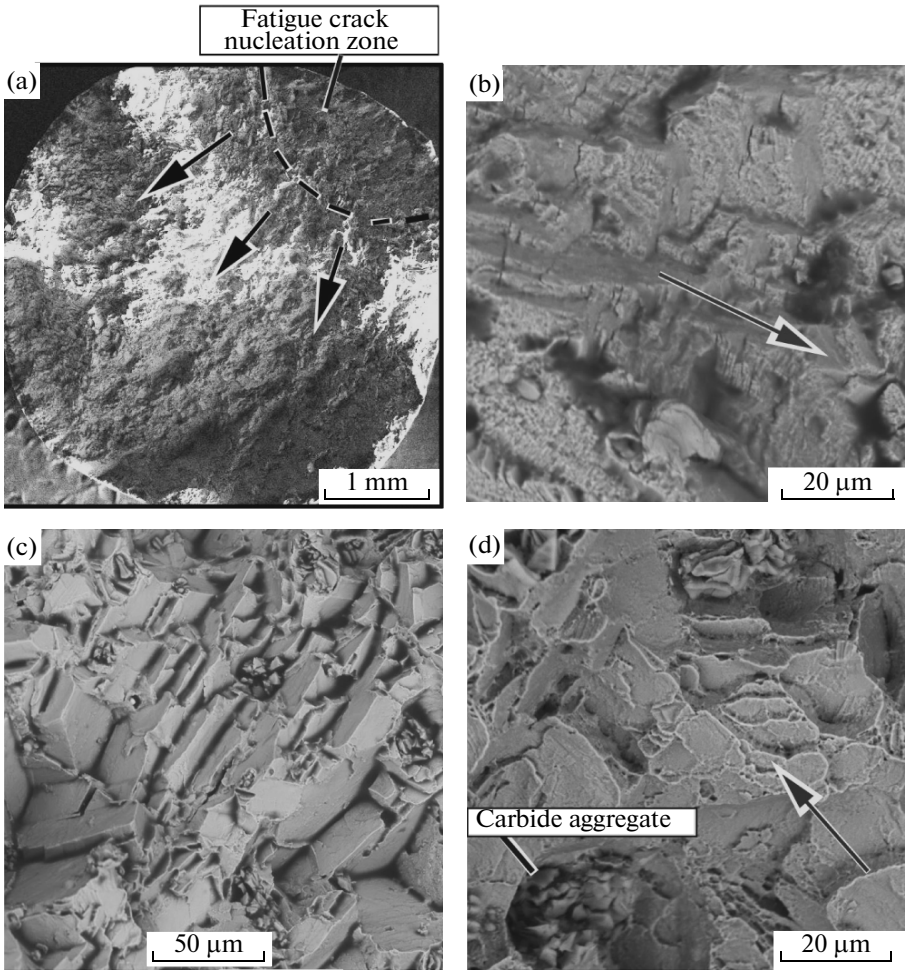

Fig. 9. Fatigue fracture surfaces of the VZh175 alloy at $T = 650°C$, $\varepsilon_a = 0.5\%$, and (a–c) $N_f = 1040$ cycles and (d) $N_f = 894$ cycles. The arrows indicate the direction of fatigue crack development.

CONCLUSIONS

The results of studying the mechanical properties of a VZh175 nickel superalloy during static tension and investigating the elastoplastic low-cycle fatigue at 20°C and an operating temperature of 650°C showed that the alloy has a high strength (σ_u = 1600 MPa at 20°C and 1530 MPa at 650°C) at a sufficient ductility (14 and 12%, respectively). When studying cyclic hardening/softening diagrams in the range ε_a = 0.4–0.6%, we found that the alloy has a sufficient stability at a test temperature of 650°C.

ACKNOWLEDGMENTS

This work was supported by the Russian Foundation for Basic Research, project no. 13-08-12084.

REFERENCES

1. *Fatigue of Materials at High Temperature* (Metallurgiya, Moscow, 1988).
2. E. N. Kablov, "Strategic trends in the development of materials and technologies of their processing up to 2030," Aviats. Matrialy i Tekhnologii, No. 8, 7–17 (2012).
3. A. A. Inozemtsev, A. M. Ratchiev, M. Sh. Nikhamkin, et al., "Low-cycle fatigue and cyclic fracture toughness of a nickel alloy under loading characteristic of turbine disks," Tyazheloe Mashinostroenie, No. 4, 30–33 (2011).
4. V. F. Terent'ev, *Fatigue of Metallic Materials* (Nauka, Moscow, 2003).
5. I. A. Birger, B. F. Balashov, R. A. Dul'nev, et al., *Structural Strength of the Materials and Parts of Gas Turbine Engines* (Mashinostroenie, Moscow, 1981).
6. O. G. Ospennikova, "Strategic trends in the development of special high-temperature alloys and steels and protective and heat-resistant coatings," Aviats. Materialy i Tekhnologii, No. 8, 19–36 (2012).
7. B. S. Lomberg, S. V. Ovsepyan, M. M. Bakradze, et al., "High-temperature nickel superalloys for gas turbine engine parts," Aviats. Materialy i Tekhnologii, No. 8, 52–57 (2012).

8. M. M. Bakradze, S. V. Ovsepyan, S. A. Shugaev, and M. N. Letnikov, "Effect of quenching on the structure and properties of EK151-ID nickel superalloy forgings," Trudy VIAM, No. 9 (2013). http://viam-works.ru

9. B. S. Lomberg, S. V. Ovsepyan, and M. M. Bakradze, "Alloying and heat treatment of nickel superalloys for next-generation gas turbine engine disks," Aviats. Materialy i Tekhnologii, No. 2, 3–8 (2010).

10. E. N. Kablov and E. R. Golubovskii, *High-Temperature Strength of Nickel Superalloys* (Mashinostroenie, Moscow, 1998).

11. E. N. Kablov, O. G. Ospennikova, and B. S. Lomberg, "Combined innovative technology of isothermal stamping of superalloy disks in air under superplasticity conditions," Aviats. Materialy i Tekhnologii, No. 8, 117–129 (2012).

12. V. F. Terent'ev and A. N. Petukhov, *Fatigue of High-Strength Metallic Materials* (IMET–TsIAM, Moscow, 2013).

13. M. S. Belyaev, M. A. Gorbovets, and T. I. Komarova, "Method for tests and the calculation determination of the fatigue limit for the horizontal segment of a fatigue curve," Aviats. Materialy i Tekhnologii, No. 3, 50–55 (2012).

14. J. Tobias, A. Chlupova, M. Petrenec, et al., "Low cycle fatigue and analysis of the cyclic stress-strain response in superalloy inconel 738LC," in *Proceedings of 18th International Conference on Engineering Mechanics, Svratka, Czech. Republic* (2012), pp. 1407–1411.

15. A. Nagesha, S. Goyal, M. Nandagopal, et al., "Dynamic strain ageing in Inconel Alloy 783 under tension and low cycle fatigue," Mater. Sci. and Eng. A **546**, 34–39 (2012).

16. V. Levkovitch, R. Sievert, and B. Svendsen, "Simulation of deformation and lifetime behavior of a FCC single crystal superalloy at high temperature under low-cycle fatigue loading," Int. J. Fatigue **28** (12), 1791–1802 (2006).

17. J. K. Wright, L. J. Carroll, J. A. Simpson, et al., "Low cycle fatigue of alloy 617 at 850°C and 950°C," J. Eng. Mater. Tech. **135** (7), 0310051–0310058 (2013).

18. V. Subramanya Sarma, M. Sundararaman, and K. A. Padmanabhan, "Effect of γ' size on room temperature low-cycle fatigue behavior of a nickel base superalloy," Mater. Sci. Tech. **14** (7), 669–675 (1998).

19. E. B. Chabina, E. V. Filonova, B. S. Lomberg, et al., "Structure of modern deformable nickel superalloys," in *All Materials. Encyclopedic Handbook* (2012), Vol. 6, pp. 22–27.

20. N. A. Makhutov, "Crack kinetics during cyclic softening," in *Strength at a Small Number of Fracture Cycles. Mechanical Fatigue Problems* (Nauka, Moscow, 1969), pp. 102–109.

Translated by K. Shakhlevich